JOURNAL OF GUIDANCE, CONTROL, AND DYNAMICS
Vol. 30, No. 4, July–August 2007

Improved Endurance of Optimal Periodic Flight

Robert H. Chen* and Jason L. Speyer†
SySense Inc., Burbank, California 91502

DOI: 10.2514/1.27313

For a class of subsonic aircraft, endurance can be improved significantly by flying in a periodic path rather than in steady state. The optimal periodic endurance problem is formulated in which the performance criterion for endurance, fuel used over flight time, is minimized and the aircraft is constrained to fly in a periodic path. The optimal steady-state endurance problem is formulated in which the instantaneous fuel rate is minimized subject to the aircraft dynamics being in equilibrium. For both optimization problems, the aircraft is further constrained to fly on the surface of a vertical cylinder. In practice, this allows the aircraft to circle above a target on the ground. Because the missions that require maximal endurance often take place in a confined airspace (e.g., surveillance, reconnaissance, and loitering before strike), this assumption appears to be more appropriate than the usual assumption in which the aircraft is constrained in a vertical plane and flies straight ahead. An example shows that for a subsonic aircraft with maximal lift-to-drag ratio of 17.4 and thrust-to-weight ratio of 0.5, the endurance of the optimal periodic flight is over three times the endurance of the optimal steady-state flight.

I. Introduction

IN NATURE, there are many examples of periodic processes such as the orbital motion of the heavenly bodies, the rhythm of the heart, and the movement of the bird's wings and the fish's tail. In contrast, many engineering systems are designed to operate in the steady-state mode, even though the performance might be improved by periodic operation. For example, the fuel efficiency of an aircraft in terms of endurance or range can sometimes be improved significantly by flying in a periodic path rather than in steady state. A review of the theoretical, numerical, and implementation literature for periodic flight is given in [1]. The basic mechanism that enables periodic flight to increase endurance over steady-state flight is that the flight condition for best aerodynamic efficiency is usually not coincident with the flight condition for best propulsion efficiency. In periodic flight, the aircraft can glide at best aerodynamic efficiency during the power-off phase and boost at best propulsion efficiency during the power-on phase. In contrast, in steady-state flight, an aircraft usually cannot fly at best aerodynamic efficiency and best propulsion efficiency simultaneously. Furthermore, an efficient kinetic-potential energy interchange also enhances the periodic performance. That is, the aircraft glides at higher altitude for a long period of time, during which there is less drag and turns on the engine near the bottom of the trajectory, to get back to higher altitude as quickly as possible. Therefore, aircraft with high lift-to-drag ratios and high thrust-to-weight ratios are generally good candidates for periodic flight aimed at increasing endurance.

In this paper, optimal periodic flight and optimal steady-state flight for endurance are investigated. In contrast to previous studies in which the aircraft is usually constrained in a vertical plane and flies straight ahead [2,3], the aircraft here is constrained to fly on the surface of a vertical cylinder (i.e., the cylinder's axis of symmetry is perpendicular to the ground plane). In this way, the aircraft's downrange versus cross range is a circle. This allows the aircraft to circle above a target on the ground. When the performance of interest is maximal range, the assumption of flying straight ahead is reasonable, because the missions that require maximal range usually concern travel between two points that are far apart. However, when the performance of interest is maximal endurance, the assumption of flying in a circle appears to be more appropriate, because the missions that require maximal endurance often take place in a confined airspace (e.g., surveillance, reconnaissance, and loitering before strike).

To formulate the optimal periodic endurance problem for aircraft that are flying in a circle, the appropriate representation of the aircraft dynamics is first derived in Sec. II. Instead of using downrange, cross range, and heading angle (which change periodically when the aircraft flies in a circle), two new states are defined that are constant no matter where the aircraft is on the circle. The first state is the ground distance between the aircraft and the center of the circle. The second state is the angle between the aircraft's velocity vector projected onto the ground and the position vector from the center of the circle to the aircraft projected onto the ground. When the aircraft flies in a circle, the first state is the radius of the circle and the second state is ± 90 deg, depending on whether the aircraft is flying clockwise or counterclockwise. The optimal periodic endurance problem is then formulated using the equations of motion associated with the altitude, velocity, flight path angle, and the two new states in Sec. III. Because the two states that describe the circular motion of the aircraft are always constant, the aircraft does not need to complete the circle in the optimal periodic endurance problem. That is, the optimal periodic trajectory can start and end anywhere on the circle. This avoids the difficulty in specifying the altitude, velocity, and flight path angle when the aircraft completes the circle. Therefore, the optimal periodic trajectory is independent of the aircraft's location on the circle. To compare the performance between the optimal periodic and steady-state flight, the optimal steady-state endurance problem is formulated in Sec. IV. Furthermore, a periodic guidance law is developed to mechanize the optimal periodic flight in Sec. V. Finally, in every section, the concept is demonstrated by the numerical example of a subsonic aircraft that has a maximal lift-to-drag ratio of 17.4 and thrust-to-weight ratio of 0.5. The optimal periodic flight will be demonstrated by autonomously flying this aircraft, which is still in development, using the periodic guidance law.

II. Aircraft Dynamics

Because the aircraft is constrained to fly on the surface of a vertical cylinder, the flight is restricted in a confined airspace. Therefore, the flat-Earth assumption can be used so that the local horizon coordinate system is an inertial coordinate system. The equations of motion for

Presented as Paper 6545 at the Guidance, Navigation, and Control Conference, Keystone, CO, 21–24 August 2006; received 15 August 2006; revision received 4 December 2006; accepted for publication 7 December 2006.

*Principal Engineer, 300 East Magnolia Boulevard, Suite 300; RobertChen@SySense.com. Senior Member AIAA.

†Chief Technology Officer, 300 East Magnolia Boulevard, Suite 300, currently Professor, University of California, Los Angeles; speyer@sysense.com. Fellow AIAA.

aircraft that perform a coordinated turn maneuver (i.e., the sideslip angle and side force are assumed zero) are then [4]

$$\dot{h} = v \sin\gamma \tag{1a}$$

$$\dot{v} = \frac{T\cos\alpha - D}{m} - g\sin\gamma \tag{1b}$$

$$\dot{\gamma} = \frac{T\sin\alpha + L}{mv}\cos\phi - \frac{g}{v}\cos\gamma \tag{1c}$$

$$\dot{r}_d = v\cos\gamma\cos\psi \tag{1d}$$

$$\dot{\psi} = \frac{T\sin\alpha + L}{mv\cos\gamma}\sin\phi \tag{1e}$$

$$\dot{r}_c = v\cos\gamma\sin\psi \tag{1f}$$

The states are the altitude h, velocity v, flight path angle γ, downrange r_d, heading angle ψ, and cross range r_c, shown in Fig. 1. The controls are the angle of attack α, thrust T, and bank angle ϕ. $L = \bar{q}S_eC_L$ is the lift, $D = \bar{q}S_eC_D$ is the drag (where $\bar{q} = \frac{1}{2}\rho v^2$ is the dynamic pressure, S_e is the reference area, and C_L and C_D are the lift and drag coefficients, respectively; and where ρ is the air density that varies with altitude), m is the aircraft mass, and g is the local acceleration due to gravity that also varies with altitude.

Instead of using r_d and r_c, two new states representing the ground distance between the aircraft and the center of the circle and the angle of the position vector from the center of the circle to the aircraft projected onto the ground are defined as

$$r \triangleq \sqrt{r_d^2 + r_c^2} \qquad \theta \triangleq \cos^{-1}\frac{r_d}{\sqrt{r_d^2 + r_c^2}}$$

and shown in Fig. 1. By using Eqs. (1d) and (1f),

$$\dot{r} = v\cos\gamma\cos(\psi - \theta) \tag{2a}$$

$$\dot{\theta} = \frac{v}{r}\cos\gamma\sin(\psi - \theta) \tag{2b}$$

Define another new state representing the angle between the aircraft's velocity vector projected onto the ground and the position vector from the center of the circle to the aircraft projected onto the ground as

$$\epsilon \triangleq \psi - \theta$$

which is also shown in Fig. 1. Equation (2) then becomes

$$\dot{r} = v\cos\gamma\cos\epsilon \tag{3a}$$

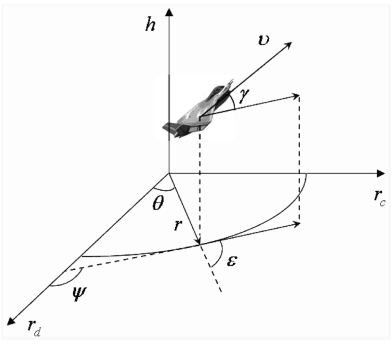

Fig. 1 Aircraft in an inertial coordinate system.

$$\dot{\theta} = \frac{v}{r}\cos\gamma\sin\epsilon \tag{3b}$$

By using Eqs. (1e) and (3b),

$$\dot{\epsilon} = \frac{T\sin\alpha + L}{mv\cos\gamma}\sin\phi - \frac{v}{r}\cos\gamma\sin\epsilon \tag{4}$$

The equations of motion for aircraft that perform a coordinated turn maneuver can now be written in terms of Eqs. (1a–1c), (3), and (4), where the states are h, v, γ, r, θ, and ϵ.

This representation of aircraft dynamics is very useful for studying aircraft that are flying in a circle, because θ, which represents the aircraft's location on the circle, does not enter into the dynamics that are associated with h, v, γ, r, and ϵ. Furthermore, the two states that describe the circular motion of the aircraft are always constant when the aircraft flies in a circle, because r is the radius of the circle and ϵ is ± 90 deg, obtained by setting Eq. (3a) to zero, depending on whether the aircraft is flying clockwise or counterclockwise. Therefore, the aircraft does not need to complete the circle in the periodic optimization problem. That is, the optimal periodic trajectory can start and end anywhere on the circle. This avoids the difficulty in specifying the altitude, velocity, and flight path angle when the aircraft completes the circle. In this way, the optimal periodic trajectory is independent of the aircraft's location on the circle and so is the periodic guidance law that is developed to mechanize the optimal periodic flight. This new formulation significantly reduces the complexity of the optimization and mechanization of periodic flight.

Remark 1: If the periodicity constraint on the altitude, velocity, and flight path angle is imposed when the aircraft completes the circle, then the ground distance traveled in one period of the optimal periodic trajectory is explicitly constrained at $2\pi r$. This would be equivalent to specifying the final downrange in the periodic optimization problem in which the aircraft is constrained in a vertical plane and flies straight ahead. Therefore, this forms a periodic optimization problem that is too conservative. This difficulty can be avoided by using the aircraft dynamics derived in this section, because the ground distance traveled in one period of the optimal periodic trajectory can now be completely free in the periodic optimization problem. Note that h, v, and γ associated with the optimal periodic trajectory will be periodic, r and ϵ will be constant, but θ will not be periodic.

The subsonic aircraft used in the numerical example of the following sections is now described in detail. Figure 2 shows a picture of the aircraft that is still in development. The takeoff weight and dry weight for the steady-state flight are 170 and 90 lb, respectively. The aerodynamics are

$$C_L = 0.1865 + 0.1062\alpha + 0.0001582\alpha^2 - 0.0001365\alpha^3 - 0.000009326\alpha^4$$

$$C_D = 0.01670 + 0.0001061\alpha + 0.0001582\alpha^2 + \frac{C_L^2}{23.7698}$$

where $-5 \le \alpha \le 10$ deg. The reference area is 30.26 ft^2. The lift-to-drag ratio is shown in Fig. 3a, with the maximum of 17.35 occurring at the angle of attack of 3.42 deg. The jet engine used by the aircraft has maximal thrust of 98.92 lb at full throttle and minimal thrust of 4.04 lb at idle. The fuel rate (in lb/h) is

Fig. 2 Aircraft for experiment and demonstration of periodic flight.

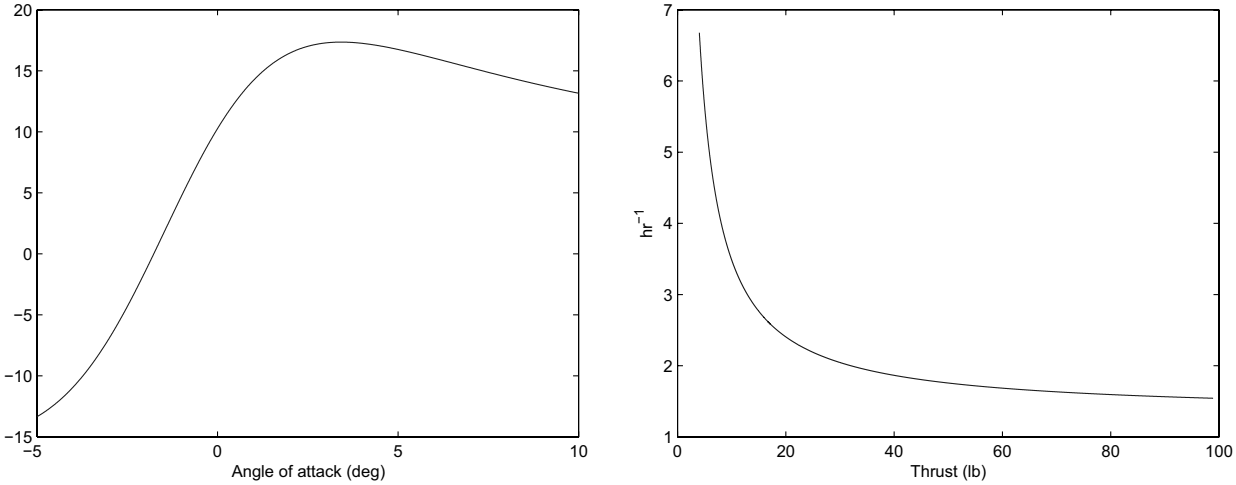

a) Lift-to-drag ratio **b) Specific fuel consumption**

Fig. 3 Aerodynamics and propulsion of the aircraft.

$$\dot{m}_f = 26.98 + 1.3244(T - 4.04)$$

The specific fuel consumption shown in Fig. 3b indicates that the best propulsion efficiency is at full throttle.

Because the aircraft turns the engine on and off during the periodic flight, its effects on the aerodynamics and propulsion of the aircraft are assumed as follows. First, when the engine is off, a drag penalty of 10% of C_D at $\alpha = 0$ is assumed. This reduces the maximal lift-to-drag ratio to 16.42, occurring at the angle of attack of 3.69 deg. Furthermore, the engine restart process is assumed to take 1 min, during which the thrust is zero and fuel rate is 26.98 lb/h, with the same drag penalty. Finally, a weight penalty of 20 lb is assumed to account for the extra equipment such as the propane used for engine restart and the extra battery for flying six hours longer than the steady-state flight, which is indicated by the results in Secs. III.B and IV.B. Therefore, the takeoff weight and dry weight for the periodic flight are 190 and 110 lb, respectively, and the thrust-to-weight ratio is 0.52.

III. Optimal Periodic Flight

A. Problem Formulation

In this section, the optimal periodic endurance problem for aircraft that are flying in a circle is formulated. First, because the aircraft is constrained to fly on the surface of a vertical cylinder, the equations of motion (1a–1c), (3), and (4) can be reduced by using this constraint. By using $\dot{r} = 0$, Eq. (3a) implies that $\epsilon = \pm(\pi/2)$, depending on whether the aircraft is flying counterclockwise or clockwise. Assume that the aircraft flies counterclockwise and $\epsilon = \pi/2$; Eq. (3b) then becomes

$$\dot{\theta} = \left(\frac{v}{r}\right)\cos\gamma \tag{5}$$

By substituting $\epsilon = \pi/2$ and $\dot{\epsilon} = 0$ into Eq. (4), the bank angle that keeps the aircraft on the circle is solved explicitly as

$$\phi = \sin^{-1}\frac{mv^2\cos^2\gamma}{r(T\sin\alpha + L)} \tag{6}$$

Therefore, the equations of motion for aircraft that are flying in a circle with a radius of r are Eqs. (1a–1c) and (5) subject to Eq. (6), where the states are h, v, γ, and θ, and the controls are α and T. Note that $r\theta$ is the ground distance traveled on the circle. By taking the limit of $r \to \infty$, Eq. (6) implies that $\phi \to 0$, and Eqs. (1a–1c) and (5) become equivalent to the equations of motion for aircraft that are constrained in a vertical plane and fly straight ahead, and $r\theta$ becomes the downrange.

The optimal periodic endurance problem is now formulated as a constrained optimization problem. The cost to be minimized is the ratio of the fuel used for flight time over one period, which is

$$J = \frac{\int_0^\tau \dot{m}_f \, \mathrm{d}t}{\tau}$$

where τ is the period. The control variables to be determined are $\alpha(t)$, $T(t)$, $h(0)$, $v(0)$, $\gamma(0)$, and τ, where $t \in [0, \tau]$. There are three types of constraints. First are the equations of motion (1a–1c) subject to Eq. (6), where r is chosen by the designer arbitrarily or in accordance with the mission's requirement. Equation (5) is not included because θ does not enter into Eqs. (1a–1c). Note that in the periodic optimization problem in which the aircraft is constrained in a vertical plane and flies straight ahead, only the limiting equations (1a–1c) are included, whereas the limiting equation (5) is not included. It is assumed that the aircraft mass is given and held fixed over the period. The aircraft mass change in one period is assumed to be negligible, because the fuel used over one period for the aircraft studied in this paper is less than 2% of the aircraft mass, as shown in Sec. III.B. This small approximation leads to an enormous savings in numerical error and computation time [5]. If the aircraft mass is not held fixed over the period, the periodicity constraints cannot be applied. Then, instead of formulating the optimization problem for a single period at a fixed aircraft mass, one has to formulate the optimization problem for the entire flight without the periodicity constraints using variable aircraft mass (i.e., given initial and final aircraft masses). Because this optimization problem does not force the trajectory to be periodic, it would be difficult to obtain the optimal trajectory that is periodic. Second are the periodicity constraints that require the initial altitude, velocity, and flight path angle to be equal to the final altitude, velocity, and flight path angle, respectively, that is, $h(\tau) = h(0)$, $v(\tau) = v(0)$, and $\gamma(\tau) = \gamma(0)$. Third are the physical constraints on the aircraft that may include limits on the altitude, velocity, angle of attack, thrust, and acceleration. For the aircraft described in Sec. II, these constraints are $-5 \le \alpha \le 10$ deg and $4.04 \le T \le 98.92$ lb when the engine is on. Furthermore, $1000 \le h \le 5000$ ft is imposed to bound the maximal and minimal altitude.

Remark 2: The optimal periodic trajectory obtained does not depend on the aircraft's location on the circle, and the aircraft may fly a fraction or multiples of the circle in one period. When the radius of the circle is chosen smaller, the lift has to be further rotated to provide more centrifugal force. Then, to generate enough upward force to counter for the gravity, the lift has to be larger, which results in larger drag. Therefore, the optimal periodic cost becomes larger when the radius of the circle becomes smaller. If the cost is also minimized with respect to the radius of the circle, then the optimal radius will simply be infinity. When the radius of the circle goes to infinity, the periodic optimization problem becomes equivalent to that in

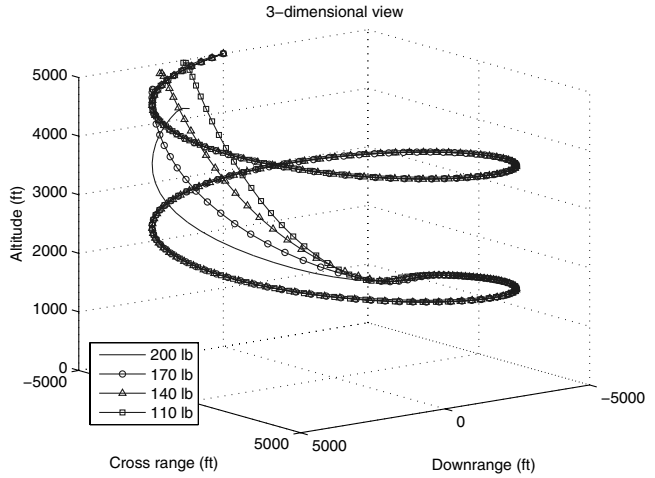

Fig. 4 Optimal periodic trajectories for different aircraft weights: three-dimensional view.

previous studies [2,3] in which the aircraft is constrained in a vertical plane and flies straight ahead.

Because the optimal periodic endurance problem is too complicated to be solved analytically, it is solved numerically by using the accelerated gradient projection method [6–9]. To implement the optimization problem into the numerical algorithm, it is divided into three phases. The first phase is the glide phase in which the engine is turned off. During this phase, the control variables are α, $h(0)$, $v(0)$, $\gamma(0)$, and τ_1 which is the flight time of the first phase. The constraints are $-5 \le \alpha \le 10$ deg and $1000 \le h \le 5000$ ft. The second phase is the engine restart phase, which lasts 60 s. During this phase, the control variable is α and the constraints are the same as those in the first phase. The third phase is the boost phase, in which the engine is turned on. During this phase, the control variables are α, T, and τ_2, which is the flight time of the third phase. The constraints are $h(\tau_1 + \tau_2 + 60) = h(0)$, $v(\tau_1 + \tau_2 + 60) = v(0)$, $\gamma(\tau_1 + \tau_2 + 60) = \gamma(0)$, and $4.04 \le T \le 98.92$ lb, in addition to those in the first phase. For details of the numerical procedure, such as the convergence criteria, please refer to [5] and the references therein. Note that this optimization problem can also be solved by using OTIS [10], which uses the sequential quadratic programming method [11,12]. However, because the focus of this paper is not comparing different numerical algorithms, only the numerical algorithm that is based on the accelerated gradient projection method is used and its performance measures, such as the number of iterations, are omitted here.

B. Numerical Results

Because the optimal periodic endurance problem assumes constant aircraft mass, the solutions are obtained for four aircraft weights at 200, 170, 140, and 110 lb, with the radius of the circle chosen as 5000 ft. The optimal periodic costs obtained are 13.15, 10.82, 8.59, and 6.60 lb/hr, respectively. Note that these solutions are only local minima and may not be the global minima. The optimal periodic trajectories for these four aircraft weights are shown in Figs. 4–6. In Fig. 4, the aircraft flies around the circle approximately twice in one period. If the radius of the circle is chosen to be much larger, then one would expect that the aircraft will fly only part of the circle in one period. In Figs. 3b and 6b, the aircraft flies at best propulsion efficiency during the boost phase, because the optimal thrust is at full throttle and the specific fuel consumption is at its minimum. In Figs. 3a and 6a, the aircraft does not fly at the angle of attack that produces the maximal lift-to-drag ratio during the glide phase. This is because the best aerodynamic efficiency for endurance for the gliding flight occurs at the angle of attack that minimizes the sink rate (i.e., $-\dot{h}$), which is different from the angle of attack that produces the maximal lift-to-drag ratio.

To demonstrate this point, an optimization problem is formulated by minimizing the sink rate for the gliding flight as

$$\min_{\alpha,v,\gamma} -v\sin\gamma$$

subject to the equations of motion in equilibrium without thrust, which is

$$0 = D + mg\sin\gamma \tag{7a}$$

$$0 = L\cos\phi - mg\cos\gamma \tag{7b}$$

where

$$\phi = \sin^{-1}\frac{mv^2\cos^2\gamma}{rL}$$

and $-5 \le \alpha \le 10$ deg. This optimization problem is solved numerically to obtain the angle of attack that minimizes the sink rate at a given altitude. Because this is a parameter optimization problem with three control variables and two equality constraints, the degree of freedom of the optimization problem is only one, and a global search method similar to the method in [5] is used to solve this optimization problem. First, by specifying the angle of attack, the velocity and flight path angle that satisfy Eq. (7) are solved numerically to obtain the cost. Then, by performing this procedure for a range of angle of attack, the cost is constructed as a one-dimensional curve versus angle of attack, and the global minimum is obtained. For example, Fig. 7 shows that the minimal sink rate between an altitude of 1000 and 5000 ft for the aircraft weight of 110 lb occurs at the angle of attack of 6.80 deg when the flight path angle is −3.84 deg and velocity is between 60.7 and 64.4 ft/s, which are very close to the optimal periodic trajectory for the glide phase in Figs. 6a, 5c, and 5b, respectively. Therefore, the aircraft flies at best aerodynamic efficiency during the glide phase.

Remark 3: To gain some insight into the angle of attack that minimizes the sink rate, the optimization problem is simplified when the aircraft is constrained in a vertical plane and flies straight ahead. Equation (7) then becomes

$$0 = \tfrac{1}{2}\rho v^2 S_e C_D + mg\sin\gamma \tag{8a}$$

$$0 = \tfrac{1}{2}\rho v^2 S_e C_L - mg\cos\gamma \tag{8b}$$

Because Eq. (8) has three variables (i.e., α, v, and γ) and two equations, it is possible to express any two variables in terms of the other variable analytically. By dividing Eq. (8a) by Eq. (8b),

$$\gamma = -\tan^{-1}\frac{C_D}{C_L}$$

Because $C_D > 0$ and C_L has to be positive from Eq. (8b), then

$$\sin\gamma = -\frac{C_D}{\sqrt{C_L^2 + C_D^2}} \tag{9}$$

By substituting Eq. (9) into Eq. (8a),

$$v = \sqrt{\frac{2mg}{\rho S_e}}\left(C_L^2 + C_D^2\right)^{-\frac{1}{4}} \tag{10}$$

If C_L and C_D are not functions of v, Eq. (9) and Eq. (10) have γ and v expressed in terms of α. The sink rate can then be expressed as

$$-\dot{h} = \sqrt{\frac{2mg}{\rho S_e}}C_D\left(C_L^2 + C_D^2\right)^{-\frac{3}{4}}$$

and plotted as a one-dimensional curve versus angle of attack at different altitude. Note that the minimal sink rate per distance is

$$-\frac{\mathrm{d}h}{\mathrm{d}r_d} = -\frac{\dot{h}}{\dot{r}_d} = -\tan\gamma = \frac{C_D}{C_L}$$

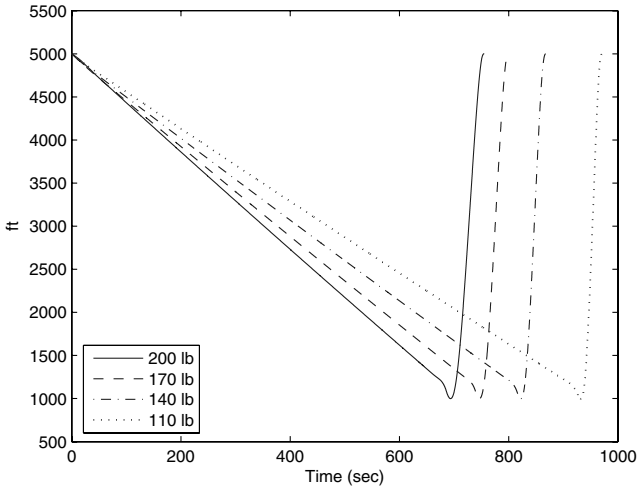

a) Altitude

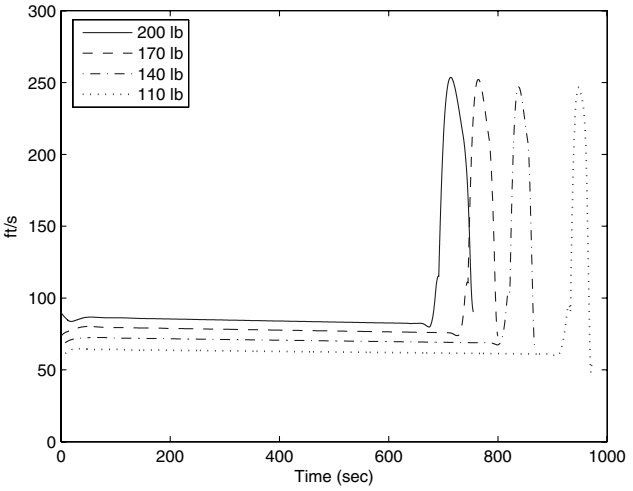

b) Velocity

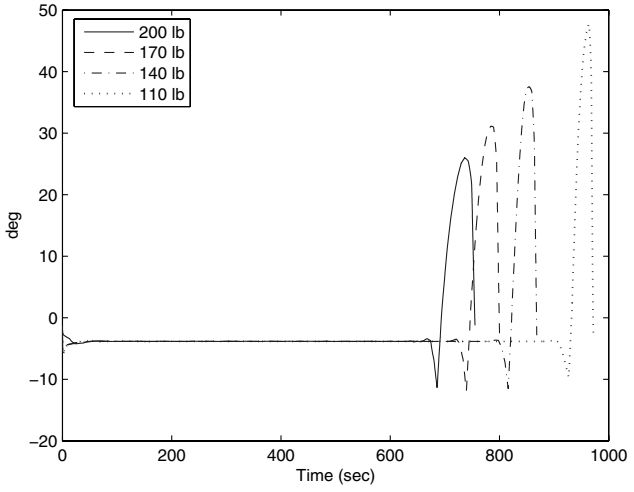

c) Flight path angle

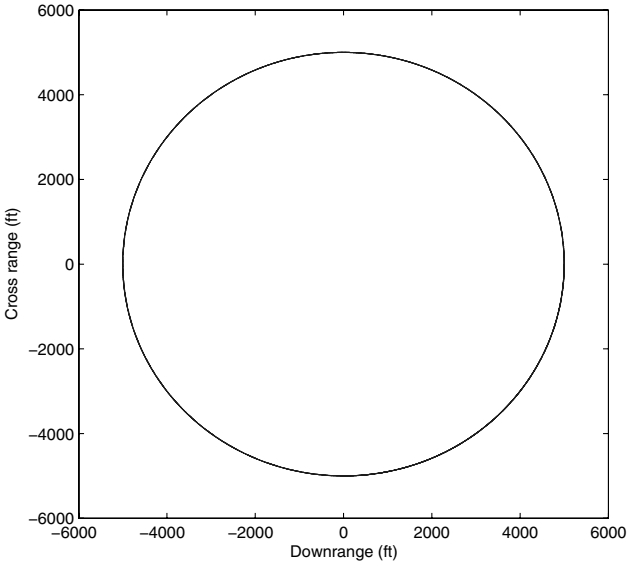

d) Overhead view

Fig. 5 Optimal periodic trajectories for different aircraft weights.

Therefore, if the performance of interest is range, the aircraft will use the angle of attack that minimizes the sink rate per distance, which is the angle of attack that produces the maximal lift-to-drag ratio. However, if the performance of interest is endurance, the aircraft will use the angle of attack that minimizes the sink rate, which is different from the angle of attack that produces the maximal lift-to-drag ratio.

Finally, the total endurance for the optimal periodic flight from the aircraft weight of 185 to 115 lb is obtained. It is assumed that the fuel required for takeoff is 5 lb and that the fuel required for landing and reserve is also 5 lb. Figure 8 shows the inverse of the optimal periodic cost versus aircraft weight. Because the total endurance is the area underneath the curve between the two aircraft weights, the total endurance for the optimal periodic flight is obtained as 7.66 h by integrating the inverse of the optimal periodic cost with respect to the aircraft weight from 115 to 185 lb.

IV. Optimal Steady-State Flight

A. Problem Formulation

In this section, the optimal steady-state endurance problem for aircraft that are flying in a circle is formulated as a constrained optimization problem in which the instantaneous fuel rate is minimized subject to the aircraft dynamics being in equilibrium and the physical constraints on the aircraft. From Eqs. (1a–1c), (3), and (4), the equations of motion in equilibrium for aircraft that are flying in a circle with radius of r are

$$0 = T\cos\alpha - D \tag{11a}$$

$$0 = (T\sin\alpha + L)\cos\phi - mg \tag{11b}$$

$$0 = (T\sin\alpha + L)\sin\phi - \frac{mv^2}{r} \tag{11c}$$

with $\gamma = 0$. Therefore, the optimal steady-state endurance problem is

$$\min_{\alpha,T,\phi,h,v} \dot{m}_f \tag{12}$$

subject to Eq. (11) and $-5 \le \alpha \le 10$ deg, $4.04 \le T \le 98.92$ lb, and $1000 \le h \le 5000$ ft. Because this is a parameter optimization problem with five control variables and three equality constraints, the degree of freedom of the optimization problem is only two, and a global search method similar to the method in [5] can be used to solve this optimization problem. First, by specifying the altitude and velocity, the angle of attack, thrust, and bank angle that satisfy Eq. (1) are solved numerically to obtain the steady-state cost. Then, by performing this procedure for a different altitude and velocity over

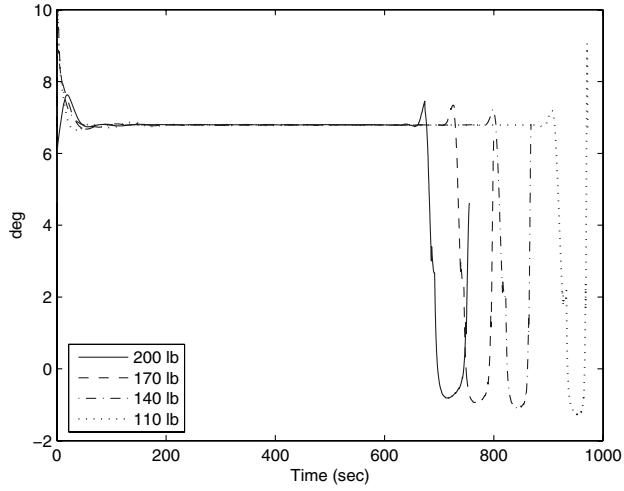

a) Angle of attack

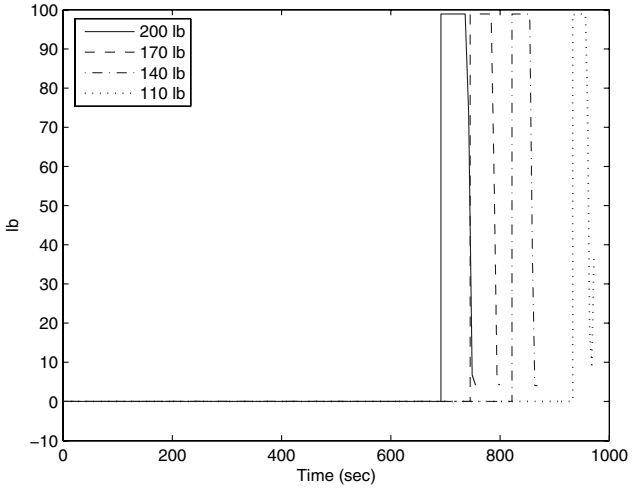

b) Thrust

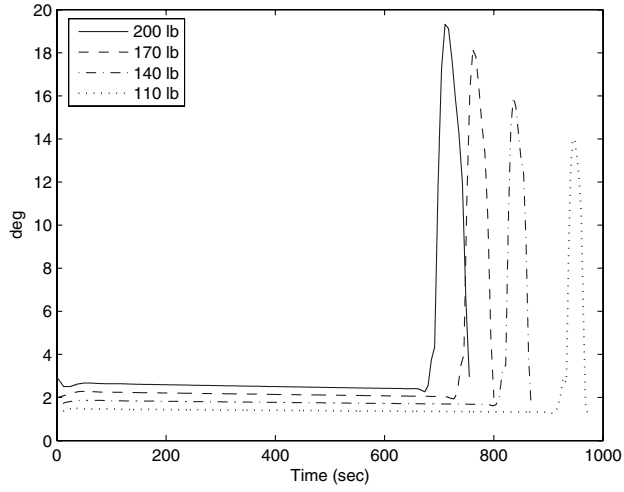

c) Bank angle

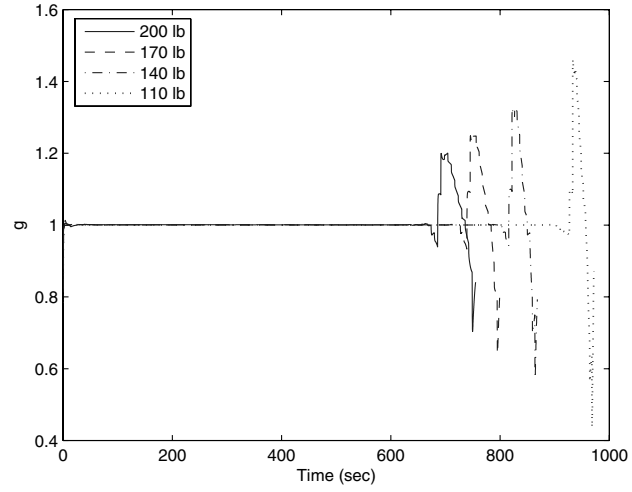

d) Net acceleration

Fig. 6 Optimal periodic trajectories for different aircraft weights.

the entire flight envelope, the steady-state cost is constructed as a two-dimensional curve versus altitude and velocity, and the global minimum is obtained.

A special case is now considered in which Eq. (11) can be solved analytically so that the computation of the numerical procedure is reduced significantly. Because Eq. (11) has five variables (i.e., α, T, ϕ, h, and v) and three equations, it is possible to express any three variables in terms of the other two variables analytically. By dividing Eq. (11c) by Eq. (11b),

$$\phi = \tan^{-1}\frac{v^2}{gr} \tag{13}$$

By using Eq. (13), Eqs. (11a) and (11b) can be written as

$$T\cos\alpha - \tfrac{1}{2}\rho v^2 S_e C_D = 0 \tag{14a}$$

$$T\sin\alpha + \frac{1}{2}\rho v^2 S_e C_L = \frac{m\sqrt{v^4 + g^2 r^2}}{r} \tag{14b}$$

By eliminating T from Eq. (14),

$$\frac{1}{2}\rho v^2 S_e(C_L\cos\alpha + C_D\sin\alpha) = \frac{m\sqrt{v^4 + g^2 r^2}}{r}\cos\alpha$$

$$\Rightarrow v = \sqrt{2mg}\left[\rho^2 S_e^2(C_L + C_D\tan\alpha)^2 - \frac{4m^2}{r^2}\right]^{-\frac{1}{4}} \tag{15}$$

By substituting Eq. (15) into Eq. (14a),

$$T = \frac{mg\rho S_e C_D}{\cos\alpha}\left[\rho^2 S_e^2(C_L + C_D\tan\alpha)^2 - \frac{4m^2}{r^2}\right]^{-\frac{1}{2}} \tag{16}$$

By substituting Eq. (15) into Eq. (13),

$$\phi = \tan^{-1}\left\{\frac{2m}{r}\left[\rho^2 S_e^2(C_L + C_D\tan\alpha)^2 - \frac{4m^2}{r^2}\right]^{-\frac{1}{2}}\right\} \tag{17}$$

If C_L and C_D are not functions of v, Eqs. (15–17) have v, T, and ϕ expressed in terms of α and h. The optimization problem (12) can then be converted into

$$\min_{\alpha,h}\dot{m}_f \tag{18}$$

subject to only inequality constraints. Because the steady-state cost can be plotted as a two-dimensional curve versus the angle of attack and altitude (e.g., Fig. 9), the global minimum within the region that satisfies the inequality constraints can be obtained by using a global

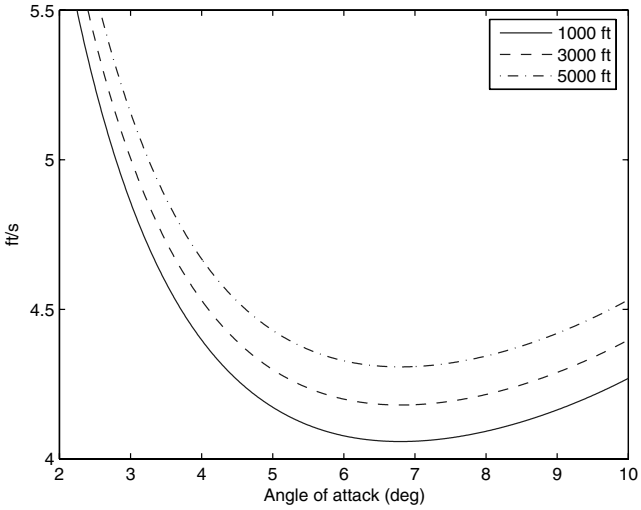

Fig. 7 Sink rate for aircraft weight of 110 lb.

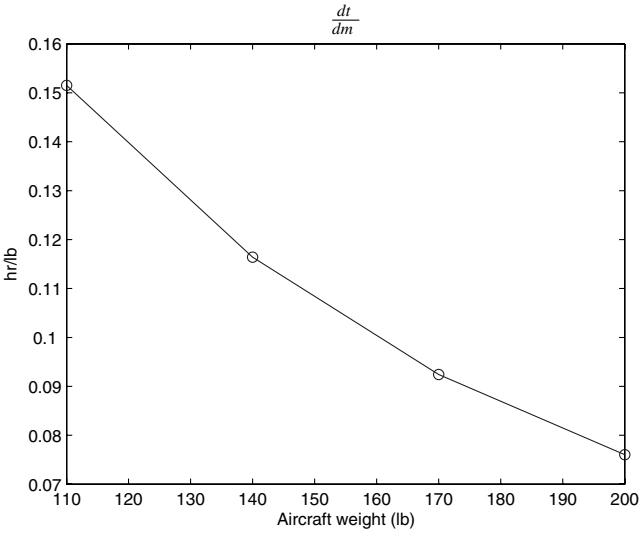

Fig. 8 Inverse of optimal periodic costs.

search method, that is, to compare the steady-state cost at a large number of different angle of attack and altitude.

Remark 4: If the aircraft is constrained in a vertical plane and flies straight ahead, by taking the limit of $r \to \infty$, Eq. (17) implies that $\phi \to 0$, and Eq. (16) becomes

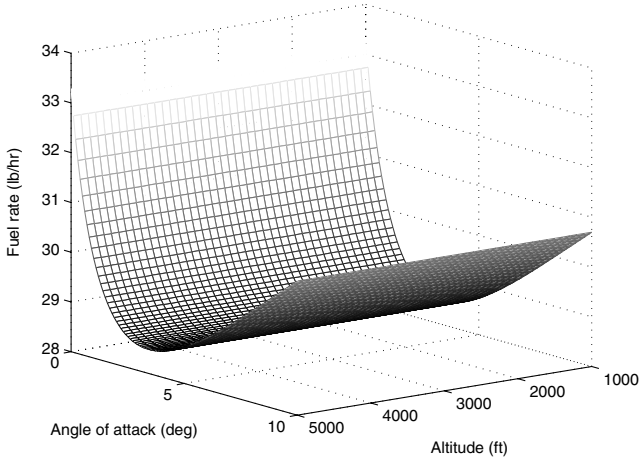

Fig. 9 Steady-state cost for aircraft weight of 90 lb.

$$\lim_{r\to\infty} T = \frac{mg}{(C_L/C_D)\cos\alpha + \sin\alpha} \tag{19}$$

If the fuel rate is linear with respect to the thrust, Eq. (19) implies that the optimal angle of attack for the optimal steady-state endurance problem is near (but not at) the angle of attack that produces the maximal lift-to-drag ratio. Note that this is the best aerodynamic efficiency for endurance for the steady-state flight. Also note that if C_L and C_D are not functions of altitude, then the steady-state cost will not be very sensitive to the altitude, as shown in Fig. 9, because the effect of the altitude only comes in through the acceleration due to the gravity.

B. Numerical Results

Because the optimal steady-state endurance problem minimizes the instantaneous fuel rate at a certain aircraft mass, the solutions are obtained for ten aircraft weights at 180, 170, 160, 150, 140, 130, 120, 110, 100, and 90 lb, with the radius of the circle chosen as 5000 ft. The optimal steady-state costs and trajectories for these ten aircraft weights are shown in Fig. 10. From Figs. 3a and 10d, the aircraft flies at best aerodynamic efficiency. From Figs. 3b and 10e, the aircraft flies far away from best propulsion efficiency. Finally, the total endurance for the optimal steady-state flight is 2.23 h, obtained by integrating the inverse of the optimal steady-state cost with respect to the aircraft weight from 95 to 165 lb.

From Sec. III.B, the total endurance of the optimal periodic flight (7.66 h) is over three times the total endurance of the optimal steady-state flight (2.23 h). Note that this result is conservative, in that the steady-state solutions are global minima, whereas the periodic solutions may only be local minima. There are three factors that contribute to the significant improvement of optimal periodic flight over optimal steady-state flight. First, in optimal periodic flight, the aircraft flies at best aerodynamic efficiency during the glide phase and best propulsion efficiency during the boost phase, whereas in optimal steady-state flight, the aircraft flies at best aerodynamic efficiency but far away from best propulsion efficiency. Second, in optimal periodic flight, the aircraft glides for a long period of time because of the high lift-to-drag ratio and boosts for a short period of time because of the high thrust-to-weight ratio. Third, by plotting the fuel rate versus thrust, as shown in Fig. 11, it is indicated that the jet engine used by the aircraft favors the periodic flight over the steady-state flight, because the curve from "engine off" to "engine idle" to "full throttle" is concave. Note that if the engine is idle instead of off during the glide phase of the periodic flight, then the optimal periodic flight will not have better endurance than the optimal steady-state flight.

V. Periodic Guidance Law

In this section, a periodic guidance law is developed (similar to the guidance law in [5]) to mechanize the optimal periodic flight. The periodic guidance law allows the constant aircraft mass assumption used for generating the optimal periodic trajectories in Sec. III.B to be removed but to retain the periodic endurance performance. For notational convenience, let the states x and controls u be

$$x \triangleq \begin{bmatrix} h & v & \gamma & r & \epsilon \end{bmatrix}^T \qquad u \triangleq \begin{bmatrix} \alpha & T & \phi \end{bmatrix}^T$$

The equations of motion (1a–1c), (3a), and (4) can then be expressed as

$$\dot{x} = f(x, u) \tag{20}$$

Denote the states and controls associated with the optimal periodic trajectory (also referred as the nominal trajectory) as x_N and u_N, respectively. Note that the nominal h, v, γ, α, T, and ϕ are periodic, whereas the nominal r and ϵ are constant. To keep the aircraft on the nominal trajectory, a periodic linear quadratic regulator is designed for each nominal trajectory.

First, the equations of motion (20) are linearized around the nominal trajectory to obtain the linearized dynamics as

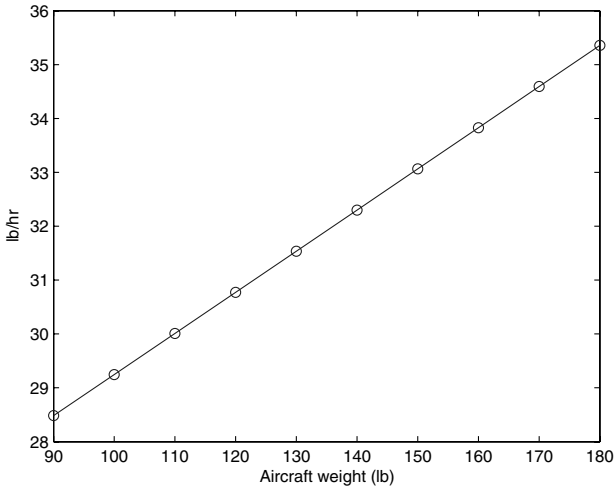

a) Optimal stead-state costs

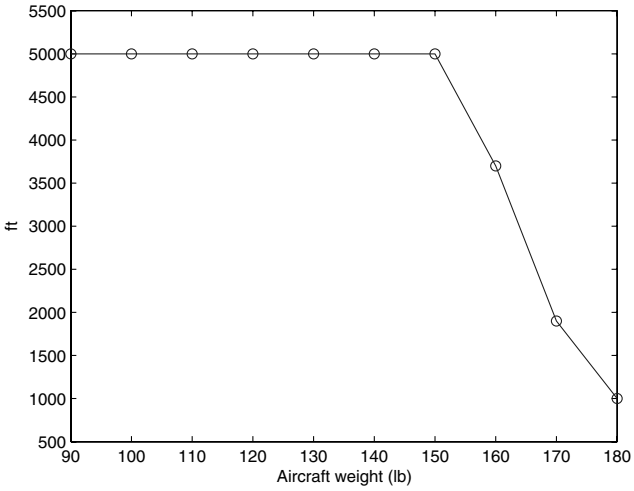

b) Altitude

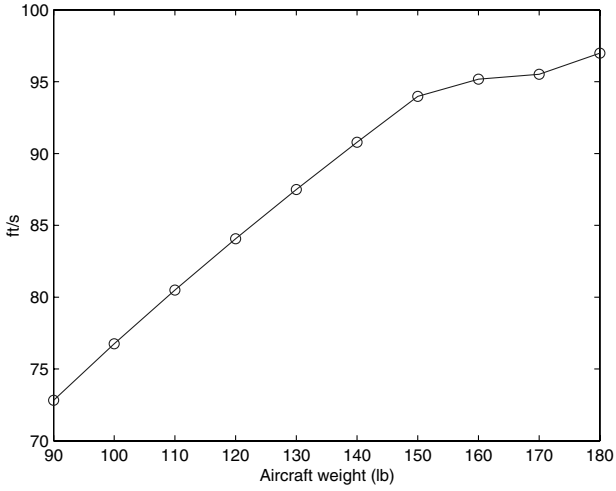

c) Velocity

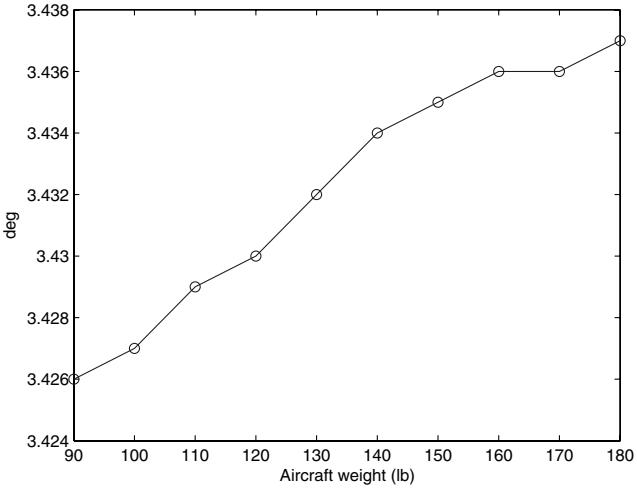

d) Angle of attack

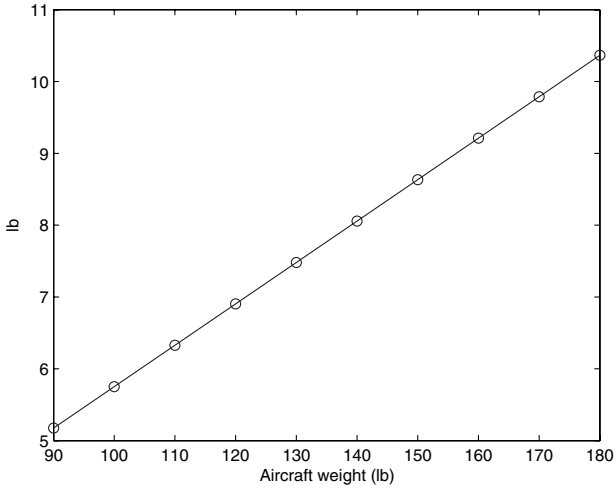

e) Thrust

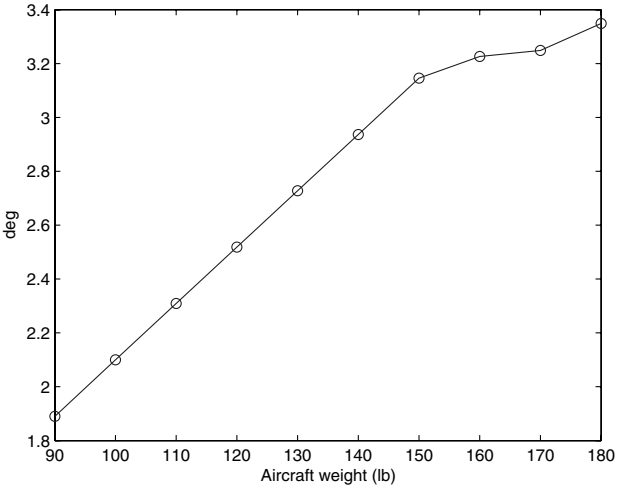

f) Bank angle

Fig. 10 Optimal steady-state trajectories for different aircraft weights.

$$\delta\dot{x}(t) = A(t)\delta x(t) + B(t)\delta u(t) \tag{21}$$

where $\delta x = x - x_N$, $\delta u = u - u_N$,

$$A = \left.\frac{\partial f}{\partial x}\right|_{x=x_N,u=u_N}, \qquad B = \left.\frac{\partial f}{\partial u}\right|_{x=x_N,u=u_N}$$

Note that the linearized dynamics are periodic because x_N and u_N are either periodic or constant. Also note that the linearized dynamics are discontinuous because the nominal thrust is discontinuous due to turning the engine on and off. The periodic linear quadratic regulator problem is then formulated as

$$\lim_{n\to\infty} \min_{\delta u(t)} \frac{1}{nT} \int_0^{nT} \frac{1}{2}[\delta x(t)^T Q \delta x(t) + \delta u(t)^T R \delta u(t)]\,\mathrm{d}t$$

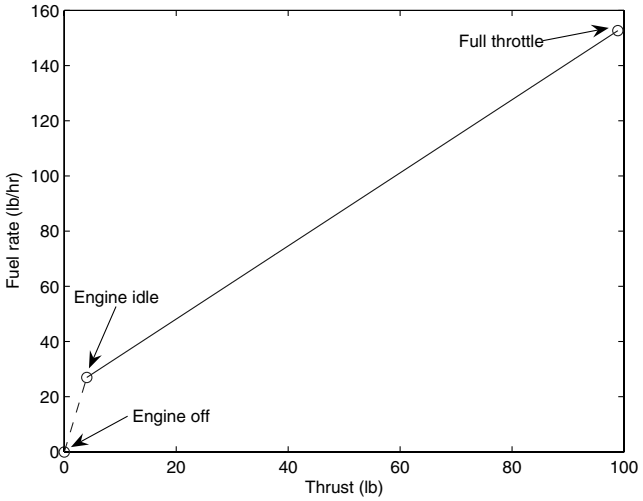

Fig. 11 Characteristic of the jet engine.

subject to Eq. (21), where $Q > 0$ and $R > 0$ are design weightings [13]. By using the calculus of variations [14], the optimal solution is

$$\delta u(t) = K(t)\delta x(t)$$

where the regulator gain is

$$K(t) = -R^{-1}B(t)^T\Pi(t)$$

and Π satisfies the periodic Riccati equation [15].

$$-\dot{\Pi}(t) = \Pi(t)A(t) + A(t)^T\Pi(t) - \Pi(t)B(t)R^{-1}B(t)^T\Pi(t) + Q, \Pi(0) = \Pi(\tau)$$

For more details about the solution around the discontinuity in the system dynamics, please refer to [5].

Because the periodic regulator is defined on the nominal trajectory and the aircraft may not be on the nominal trajectory, an index point is defined from which the nominal values (i.e., x_N, u_N, and K) required for the periodic regulator are retrieved. The index point is defined as the point on the nominal trajectory for which the h, v, and γ are closest to the current h, v, and γ in terms of certain criterion. Note that r and ϵ are not included because they are constant on the nominal trajectory. Then, by indexing the nominal trajectory with time, the

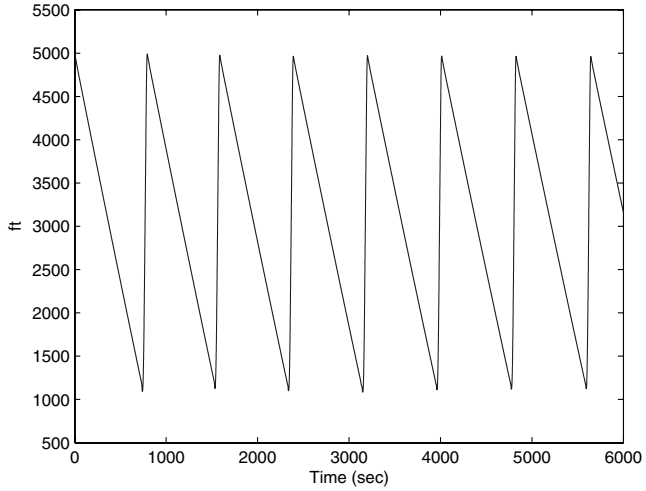

a) Altitude

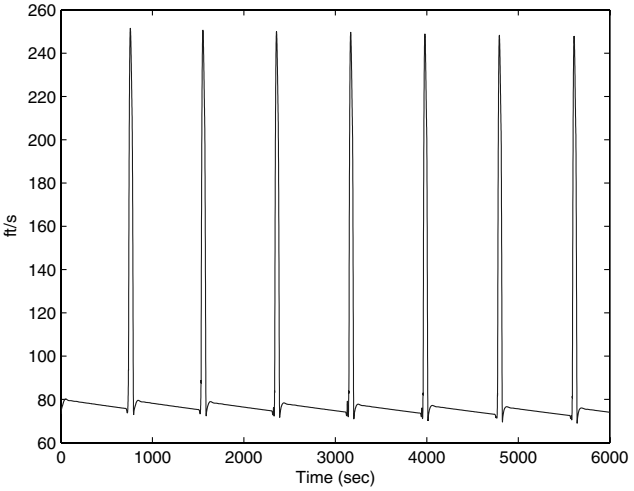

b) Velocity

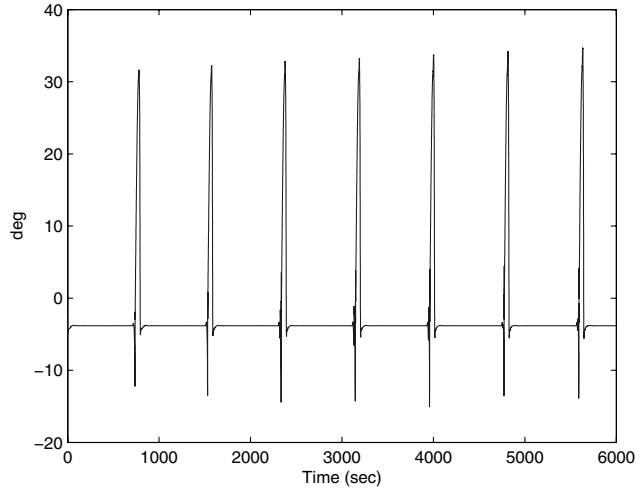

c) Flight path angle

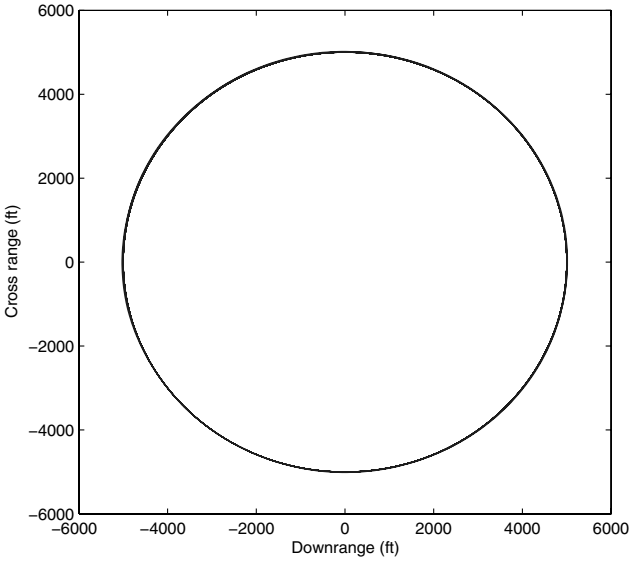

d) Overhead view

Fig. 12 Optimal periodic flight.

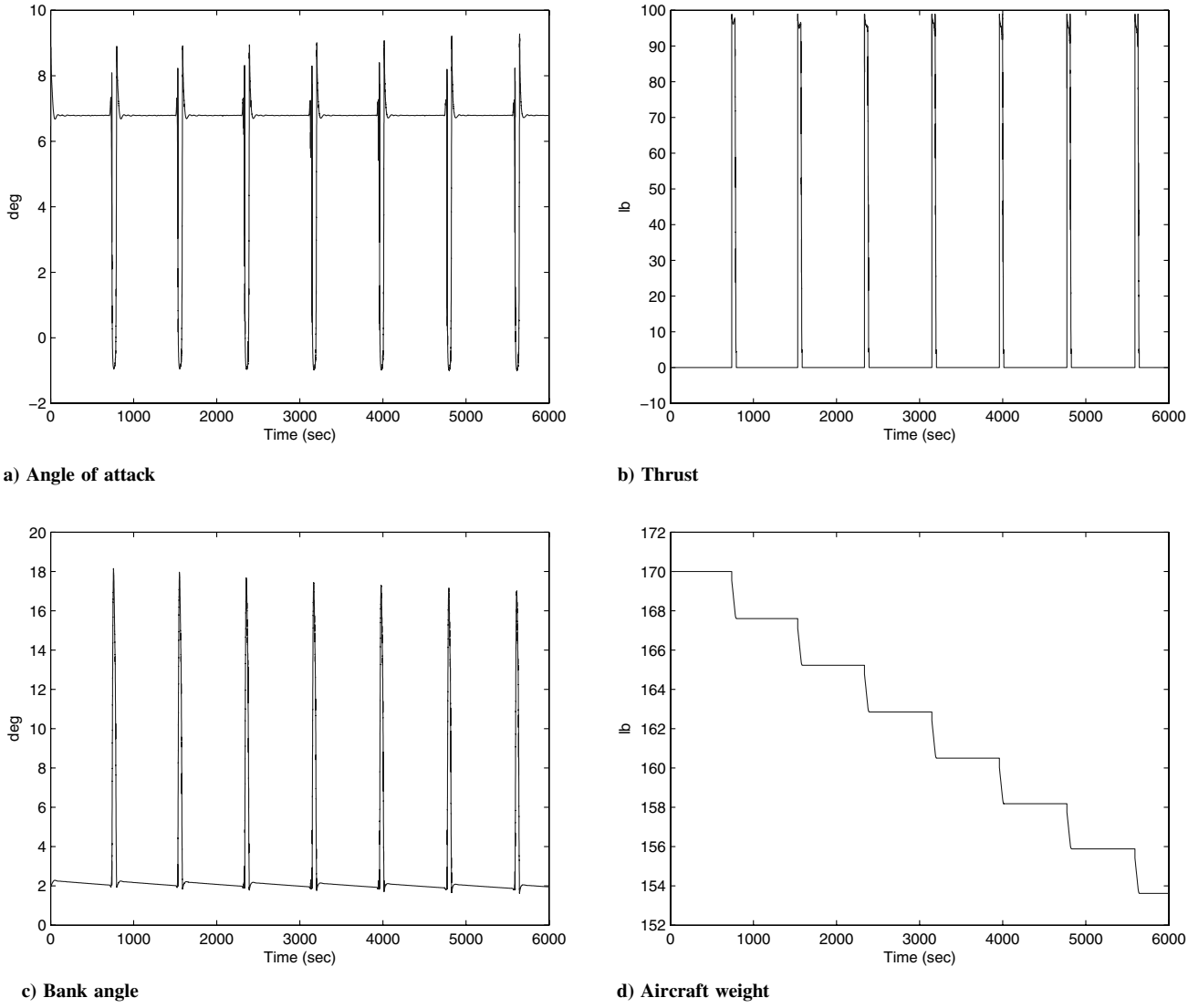

a) Angle of attack **b) Thrust**

c) Bank angle **d) Aircraft weight**

Fig. 13 Optimal periodic flight.

index time t_I of the index point can be obtained by solving an optimization problem [5]. After using the current h, v, and γ to determine t_I, x_N, u_N, and K can be obtained to generate u that will keep the aircraft on the nominal trajectory. After designing the periodic regulators for a group of optimal periodic trajectories associated with a range of aircraft mass, the periodic guidance law is constructed based on these periodic regulators to handle the decreasing aircraft mass [5]. Essentially, x_N, u_N, and K are obtained by linearly interpolating between those for the next heavier and lighter aircraft masses using the current aircraft mass. For more details, please refer to [5].

Finally, the periodic guidance law is implemented to mechanize the optimal periodic flight. The periodic guidance law is constructed based on four periodic regulators designed at the aircraft weight of 200, 170, 140, and 110 lb. The optimal periodic flight mechanized by the periodic guidance law from aircraft weight of 170 to 153.6 lb is shown in Figs. 12–14. By comparing the periodic trajectory generated by using the periodic guidance law in Fig. 12 to the optimal periodic trajectories generated for four aircraft weights in Fig. 5, the periodic guidance law tracks the optimal periodic trajectories very well, even though the aircraft weight decreases because of fuel consumption.

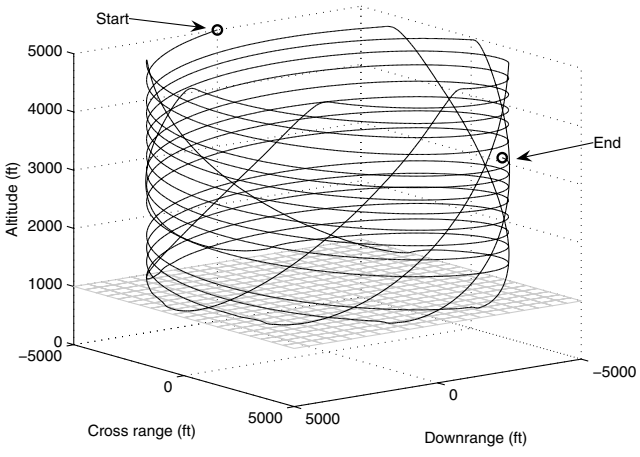

Fig. 14 Optimal periodic flight: three-dimensional view.

VI. Conclusions

The optimal periodic and steady-state endurance problems are formulated and solved for aircraft that are flying in a circle. An example shows that for a subsonic aircraft with a maximal lift-to-drag ratio of 17.4 and thrust-to-weight ratio of 0.5, the endurance of the optimal periodic flight is over three times the endurance of the optimal steady-state flight. It is also shown that the optimal periodic flight can be mechanized by the periodic guidance law.

References

[1] Speyer, J. L., "Periodic Optimal Flight," *Journal of Guidance, Control, and Dynamics*, Vol. 19, No. 4, July–Aug. 1996, pp. 745–755.

[2] Sachs, G., and Christodoulou, T., "Endurance Increase by Cyclic Control," *Journal of Guidance, Control, and Dynamics*, Vol. 9, No. 1, 1986, pp. 58–63.

[3] Sachs, G., and Christodoulou, T., "Reducing Fuel Consumption of Subsonic Aircraft by Optimal Cyclic Cruise," *Journal of Aircraft*, Vol. 24, No. 9, 1987, pp. 616–622.

[4] Miele, A., *Flight Mechanics*, Addison–Wesley, Reading, MA, 1962, pp. 42–50.

[5] Chen, R. H., Williamson, W. R., Speyer, J. L., Youssef, H., and Chowdhry, R., "Optimization and Implementation of Periodic Cruise for a Hypersonic Vehicle," *Journal of Guidance, Control, and Dynamics*, Vol. 29, No. 5, Sept.–Oct. 2006, pp. 1032–1040.

[6] Speyer, J. L., Kelley, H. J., Levine, N., and Denham, W. F., "Accelerated Gradient Projection Technique with Application to Rocket Trajectory Optimization," *Automatica*, Vol. 7, No. 1, Jan. 1971, pp. 37–43.

[7] Rosen, J. B., "The Gradient Projection Method for Nonlinear Programming, Part 1: Linear Constraints," *Journal of the Society for Industrial and Applied Mathematics*, Vol. 8, No. 1, 1960, pp. 181–217.

[8] Rosen, J. B., "The Gradient Projection Method for Nonlinear Programming, Part 2: Nonlinear Constraints," *Journal of the Society for Industrial and Applied Mathematics*, Vol. 9, No. 4, 1961, pp. 514–532.

[9] Fletcher, R., and Powell, M. J. D., "A Rapidly Convergent Descent Method for Minimization," *Computer Journal*, Vol. 6, No. 2, 1963, pp. 163–168.

[10] Hargraves, C. R., and Paris, S. W., "Direct Trajectory Optimization Using Nonlinear Programming and Collocation," *Journal of Guidance, Control, and Dynamics*, Vol. 10, No. 4, July–Aug. 1987, pp. 338–342.

[11] Gill, P. E., Murray, W., and Saunders, M. A., "SNOPT: An SQP Algorithm for Large-Scale Constrained Optimization," *SIAM Journal on Optimization*, Vol. 12, No. 4, 2002, pp. 979–1006.

[12] Betts, J. T., *Practical Methods for Optimal Control Using Nonlinear Programming*, Society for Industrial and Applied Mathematics, Philadelphia, 2001, pp. 28–30.

[13] Bittanti, S., Laub, A. J., and Willems, J. C. (ed.), *The Riccati Equation*, Springer–Verlag, Berlin, 1991, pp. 127–162.

[14] Bryson, A. E., Jr., and Ho, Y.-C., *Applied Optimal Control: Optimization, Estimation, and Control*, Hemisphere, New York, 1975, pp. 148–153.

[15] Shayman, M. A., "On the Phase Portrait of the Matrix Riccati Equation Arising from the Periodic Control Problem," *Journal of Control and Optimization*, Vol. 23, No. 5, Sept. 1985, pp. 717–751.